DRAFT VERSION FEBRUARY 1, 2008
Preprint typeset using LaTeX style emulateapj v. 25/04/01

OBSERVATIONAL EVIDENCE FOR A MULTIPHASE OUTFLOW IN QSO FIRST J1044+3656

JOHN EVERETT[1], ARIEH KÖNIGL[1,2], AND NAHUM ARAV[3,4]
Accepted for publication in ApJ v569 n2, April 20, 2002

ABSTRACT

Spectral absorption features in active galactic nuclei (AGNs) have traditionally been attributed to outflowing photoionized gas located at a distance of order a parsec from the central continuum source. However, recent observations of QSO FIRST J104459.6+365605 by de Kool and coworkers, when intepreted in the context of a single-phase gas model, imply that the absorption occurs much farther (≈ 700 pc) from the center. We reinterpret these observations in terms of a shielded, multiphase gas, which we represent as a continuous low-density wind with embedded high-density clouds. Our model satisfies all the observational constraints with an absorbing gas that extends only out to ~ 4 pc from the central source. The different density components in this model coexist in the same region of space and have similar velocities, which makes it possible to account for the detection in this source of absorption features that correspond to different ionization parameters but have a similar velocity structure. This model also implies that only a small fraction of the gas along the line of sight to the center is outflowing at the observed speeds and that the clouds are dusty whereas the uniform gas component is dust free. We suggest that a similar picture may apply to other sources and discuss additional possible clues to the existence of multiphase outflows in AGNs.

Subject headings: galaxies: active — galaxies: Seyfert — quasars: absorption lines — quasars: individual (FIRST J104459.6+365605) — MHD

1. INTRODUCTION

Modeling active galactic nuclei (AGNs) is a challenging endeavor in part because of the uncertain geometry of the gas and dust within their cores. Our best understanding of the gas distribution comes from reverberation mappings (Blandford & McKee 1982; Netzer & Peterson 1997), which indicate that the broad emission-line region (BELR) lies at a distance $R_{\rm BELR} \approx 0.01 L_{44}^{1/2}$ pc from the central continuum, where L_{44} is the luminosity in the spectral band $\sim 0.1-1$ μm in units of 10^{44} ergs s^{-1}. Based on observed absorption of BELR features by broad absorption-line region (BALR) gas and on optical polarization measurements, it has been inferred that the BALR lies outside of the BELR; the best estimates have placed the BALR somewhere between a few tenths and several parsecs from the central source (e.g., Turnshek 1988).

Velocities for these outflows are well determined from Doppler shifts: the BELR and BALR components have speeds $\lesssim 5000$ to 8000 km s^{-1} and $\lesssim 30000$ km s^{-1}, respectively. Other outflow components have also been detected. Observations of the "warm absorber" (a partially ionized X-ray absorbing gas) in Seyfert galaxies and radio-quiet QSOs, and of a UV-absorbing component apparently associated with the warm absorber, indicate gas outflowing at $\lesssim 10^3$ km s^{-1}. Furthermore, spectral lines classified as being from the Narrow Line Region (NLR) correspond to velocities of $\lesssim$ several hundred km s^{-1}.

Different theories have been proposed to explain some of these outflows. For example, Emmering, Blandford, & Shlosman (1992) considered a hydromagnetically-driven disk outflow of discrete, long-lived clouds as a model of the BELR, whereas Murray et al. (1995) and Proga, Stone, & Kallman (2000) explored radiatively-driven, continuous disk winds as the origin of the BELR and the BALR. These models all involved a single-phase gas medium.

Recently, de Kool et al. (2001, hereafter dK01) analyzed a Keck HIRES spectrum of the FIRST Bright Quasar Source J104459.6+365605 (hereafter, FBQS 1044). They inferred that excited Fe II levels are not populated according to local thermodynamic equilibrium. This observation implies an electron number density $n_e \approx 4 \times 10^3$ cm^{-3}, which, together with the observed broad absorption in Mg II [qualifying this object as a broad absorption-line quasar (BALQSO)], the Mg I absorption features, and single gas-phase photoionization models, place this BALR at ~ 700 parsecs from the central source.

Not only does this surprising result contradict the picture of a close-in BALR, but, in addition, dK01's thorough analysis suggests that the gas only partially covers the continuum source. It is not easy to understand how the absorbing gas could be approximately 1 kpc from the center and yet only partially cover the AGN core. Additionally, the Keck spectra indicate distinct groupings of gas in velocity space; it is also difficult to explain how these apparent clumps could move to such a large distance and still remain bunched up, retaining distinct identities. Even more striking is dK01's observation that different ionization states have a similar kinematic structure (i.e., residual intensity as a function of velocity): in particular, both Fe II and Mg I exhibit absorption troughs at -200, -1250, -3550, and -3800 km s^{-1}.

The 700 pc distance estimate results from combining the ionization parameter[5] implied by the observed low-ionization Mg and Fe absorption lines with the inferred values of n_e and L ($= 10^{46}$ergs s^{-1}). One can reduce this distance estimate by atten-

[1] Department of Astronomy and Astrophysics, University of Chicago, 5640 S. Ellis Avenue, Chicago, IL 60637, I:everett@jets.uchicago.edu
[2] Enrico Fermi Institute, University of Chicago, I:arieh@jets.uchicago.edu
[3] Astronomy Department, UC Berkeley, Berkeley, CA 94720, I:arav@astron.Berkeley.EDU
[4] Physics Department, University of California, Davis, CA 95616

[5] The ionization parameter $U \equiv Q/4\pi nr^2 c$ is the dimensionless ratio of the hydrogen-ionizing photon density to the hydrogen number density n: Q is the rate of incident hydrogen-ionizing photons, r is the distance from the continuum source, and c is the speed of light.

uating the incident continuum by an intermediate gas "shield." In this model, however, ions at different ionization states (such as the Fe II and Mg I components seen in FBQS 1044) are expected to occupy different regions in space, with lower values of U corresponding to larger distances from the center (e.g., Voit, Weymann, & Korista 1993). This stratification will likely lead to disparate velocities for the different ions: for example, models of self-similar MHD winds and of radiatively-driven constant-U outflows predict that the terminal velocity, v_∞, varies as $r_{\rm inject}^{-1/2}$, where $r_{\rm inject}$ is the radius at which the gas is injected into the outflow (e.g., Blandford & Payne 1982; Arav, Li, & Begelman 1994). Models that rely solely on shielding and distance to separate the different ionization components therefore cannot explain dK01's observations, in which different ionization states are found to have similar velocities.

We propose to explain the observations of FBQS 1044 by generalizing the single-phase shielded-gas model, attributing the different ionization states to different density components in a multiphase outflow. These components coexist at the same distance from the center and thus have different ionization parameters but essentially the same velocities. In particular, if the high- and low-ionization lines arise, respectively, in a continuous wind and in dense clouds that are embedded in the outflow, then all the absorption components produced in a given region of the wind will exhibit similar kinematic signatures.

In our model, the continuous gas component extends from near the black hole's event horizon out to the distance where the observed Fe II absorption and electron density can be reproduced. The inner part of this component (interior to the BALR) is identified as the "shield." This region could be associated with an MHD-driven (Königl & Kartje 1994), a Thomson scattering-driven (e.g., Blandford 2001), or a "failed" line-driven (e.g., Murray et al. 1995; Proga, Stone, & Kallman 2000) disk wind, or with a disk corona (e.g., Emmering et al. 1992). The outer region of the continuous gas component is outflowing and accounts for the Fe II and Mg II absorption, but is still too highly ionized to contain Mg I absorbing gas. Within this outflow are embedded higher-density clouds that account for the lower-ionization Mg I absorption: their high density yields a lower U in the clouds, allowing Mg I to exist. Such a two-component outflow may arise naturally in the context of a centrifugally driven disk wind, which could uplift clouds from the disk surface by its ram pressure and confine them by its internal magnetic pressure (e.g., Emmering et al. 1992; Kartje et al. 1999; Everett, Königl, & Kartje 2001). Alternatively, the clouds may represent transient density enhancements that are produced by turbulence (e.g., Bottorff & Ferland 2001) or by shocks in a radiatively driven wind (e.g., Arav et al. 1994). For illustration, we adopt here the "clouds uplifted and confined by an MHD wind" picture.

2. MULTIPHASE OUTFLOW MODEL

2.1. *Setup*

Our model consists of two segments that represent two distinct gas phases. The first segment, which corresponds to the continuous phase, extends from $r_{\rm in} = 10\,GM/c^2 = 7.4\times10^{13}$ cm (following dK01, we take the central black-hole mass to be $M = 5\times10^8 M_\odot$) out to just past the hydrogen recombination front, which corresponds to the Fe III $\rightarrow$ Fe II transition. The second segment, which models the confined dense clouds, is a constant-density zone located just beyond the continuous gas component (since the cloud temperature is nearly uniform, this provides a good representation of magnetically confined constant-pressure clouds). In reality, the continuous outflow in the line-absorption region can be expected to engulf the clouds, but this simplified model should capture the basic physical effects of a two-phase medium. (We verified that our results are independent of the cloud radial distribution within the Fe II/Mg I absorption region.)

We obtain the ionization structure of the different gas phases using the photoionization code Cloudy (Ferland 2000), adopting the same source parameters as in dK01 and assuming (as they do in most of their models) a Mathews & Ferland (1987) spectrum. We take the scaling of the hydrogen number density with spherical radius to be $n(r)\propto r^{-1}$, as in the AGN disk-wind models considered by Königl & Kartje (1994). In these self-similar MHD outflows, the magnetic field $B_{\rm wind}$ also scales as r^{-1}, which results in magnetically confined clouds having a constant ionization parameter.

We first calculate the photoionization of the continuous component, stopping the computation when n_e drops to 4×10^3 cm^{-3} (the value inferred from the observations). We then calculate how the radiation emerging through the continuous segment affects clouds located at that distance. The two parameters we adjust in our model are $n_{w,i}$, the wind hydrogen number density at $r_{\rm in}$, and n_c, the hydrogen number density of the clouds. We explore a range of models to find the values of $n_{w,i}$ and n_c that best reproduce the observations.

2.2. *Results*

Our best-fit value for the wind density is $n_{w,i}\approx10^{8.75}$ cm^{-3}. This yields the observed n_e in the region (at $r\approx4$ pc) where the Fe II column density in the wind attains the observed value of 3×10^{15} cm^{-2}, which is significant since the n_e measurement comes from the Fe II absorption lines. However, we do have to cut off the outflow very close to the end of the hydrogen recombination front so as not to exceed the observed Fe II column (see Fig. 1). Although the abrupt end of the absorbing column could be an artifact caused by our simplified treatment, the occurrence of a strong reduction in the absorption at this location may have an actual physical basis. It may be a consequence of the decrease in the ionization fraction in this region, which reduces the efficiency with which the disk can drive an MHD outflow, and it may also reflect a transition from a gaseous to a "clumpy" disk (see Shlosman & Begelman 1987) or from differential to solid-body disk rotation (see Bottorff, Korista, & Shlosman 2000) on that scale.

We also note from Figure 1 that the Mg II front occurs ~2.5 times closer to the central source than the Fe II front. (This is due to the formation of a He III $\rightarrow$ He II front in the wind that absorbs photons with E $>$ 54.4 eV, allowing Mg III, with an ionization energy of 80.1 eV, to recombine into Mg II.) Since $v_\infty\propto r_{\rm inject}^{-1/2}$ in our chosen disk-wind model (see §1), the predicted smaller initial radius of the Mg II front is consistent with the higher Mg II velocities observed in FBQS 1044.

Besides determining the measured values of the Fe II column and of n_e, the continuous wind component in our model also exerts a strong influence on the cloud absorption properties through its effect on the transmitted continuum spectrum. We find that, in order for the clouds to account for the observed Mg I absorption without also dominating the Fe II absorption, their iron gas-phase abundance must be reduced, which we attribute to depletion by dust. We assume an ISM dust composition [the default Cloudy graphite and silicate grains with a

Mathis, Rumpl, & Nordsieck (1977; hereafter MRN) power-law size distribution]. The dust abundance is constrained by the measured extinction: $A_{2500} \lesssim 1.0$.

Our best-fit value for the typical cloud density is $n_c \approx 10^{8.5}$ cm^{-3}. This means that the clouds are $\sim 10^4$ times denser (and have a correspondingly lower ionization parameter) than the surrounding continuous wind. Figure 2 shows the absorption column densities associated with a string of such clouds as a function of pathlength through the clouds.

Our model can account for the observations with cloud densities that range between $10^{7.75}$ and 10^9 cm^{-3}. This leeway reflects the uncertainty in A_{2500}. Whereas dK01 employ an extinction of 1.0 magnitude, A_{2500} could range from ~ 1.0 down to 0.2 magnitudes based on a comparison between the spectrum of FBQS 1044 and that of an "average" QSO (Weymann et al. 1991). If a population of lower-density clouds were present with a significant fraction of the observed Mg I column, then the dusty clouds would have $A_{2500} > 1$. On the other hand, if $n_c \gg 10^9$ cm^{-3}, A_{2500} would drop below 0.25. With $n_c = 10^{8.5}$ cm^{-3} we predict $A_{2500} \approx 0.5$ magnitudes, which fits well within the inferred range.

With the extinction already accounted for, the data require the continuous gas component to be effectively dust free. We tested this hypothesis by including Cloudy's Orion-type dust (a set of graphite and silicate grains with MRN's minimum size increased from 0.0025 to 0.03 μm, appropriate to a UV-irradiated medium) in the wind, taking into account dust sublimation and sputtering. To include the effects of the latter process, we removed all dust grains whose sputtering time scales (calculated following Tielens et al. 1994) do not exceed 1000 yr (the approximate time grains spend in the wind if they travel at the observed outflow velocity over a distance of 1 pc). Including both of these effects, the predicted dust extinction is over one order of magnitude greater than the maximum value allowed by the observations. We also considered the effect of changing the scaling of the wind density with radius from $n \propto r^{-1}$ to $n \propto r^{-3/2}$ (as in Blandford & Payne 1982) and to $n \propto r^{-2}$. These models again overestimate the extinction by about an order of magnitude after dust sublimation and sputtering are taken into account. We therefore conclude that, if the gas comprising the shield is associated with a disk outflow, then it must already be dust free when it leaves the disk. Such a situation could arise if the wind originates in a hot disk corona where the matter resides long enough for any dust grains to be destroyed.

However, to provide the requisite shielding, a dust-free wind requires a higher total gas column than a dusty outflow, so the inferred lack of dust in the wind implies a prohibitively large mass outflow rate — much larger than could be launched by the magnetic field that confines the clouds in our model. Thus, only part of the shield can be outflowing at velocities that are comparable to (or exceed) the observed speeds. Perhaps the inner outflow has a lower velocity than we predict, or else some of the shield may not even be outflowing, as in a disk corona or a "failed" line-driven wind (see §1).

All of these considerations yield our best model, which is compared with the observational results in Table 1. This model satisfies all the observational constraints and implies that the absorbing gas lies over two orders of magnitude closer to the central source than the earlier estimate. The radius where the observed gas leaves the disk surface is, in general, smaller yet.

We can estimate the mass outflow rate associated with the absorbing gas through the relation $\dot{M}_{\rm wind} \approx 2\pi r f N_{\rm H} m_p v$, where f is the fraction of 4π steradians into which the wind flows, $N_{\rm H}$ is the total hydrogen column density of *only* the inferred Mg II and Fe II absorbing region ($\approx 3.9 \times 10^{23}$ cm^{-2}), v is the observed outflow speed ($\sim 10^8$ cm s^{-1}), r ($= 1.2 \times 10^{19}$ cm) is the inferred distance, and where we assume a vertically and azimuthally continuous wind. We take $f \sim 0.1$ for BALQSO sources (Weymann 1997). For the above values, we find $\dot{M}_{\rm wind} \approx 8\ M_\odot$ yr^{-1}.

By equating the thermal pressure in the clouds ($\approx 2.7 \times 10^{-4}$ dynes cm^{-2}) to the confining wind magnetic pressure, $B^2_{\rm wind}/8\pi$, we deduce $B_{\rm wind} \approx 8.2 \times 10^{-2}$ G. It is encouraging that, when this value of $B_{\rm wind}$ is used in the $n(r) \propto r^{-1}$ self-similar MHD wind model, it implies a local mass outflow rate that is comparable to the above estimate of $\dot{M}_{\rm wind}$, yielding $\sim 4\ M_\odot$ yr^{-1}. If we instead choose $n_c = 10^9$ cm^{-3} (so as to satisfy the lower limit on the dust extinction, $A_{2500} = 0.25$) and require pressure balance, we find $\dot{M}_{\rm wind} \approx 9\ M_\odot$ yr^{-1}.

3. CONCLUSION

The most robust result of our study is that a shielded, multiphase absorption region reproduces the observations of FBQS 1044 on a conventional BALR scale (≈ 4 pc). In addition, when one attributes the Fe II and Mg II absorption to a low-density outflow component and the Mg I absorption to a cospatial high-density outflow component, it is possible to explain the similar kinematic structure of the respective spectral features. We also find that only a small fraction of the gas along the line of sight can be outflowing at the observed speeds and that only the high-density component of the outflow is dusty. We derived these results using a "clouds embedded in a continuous MHD disk wind" model, but our conclusions also apply to other plausible scenarios that include a continuum-shielding gas column and an absorption region that contains distinct low- and high-density components. Our basic conclusions appear to be quite general, although the precise composition of the absorbing gas and its detailed spatial and kinematic properties are not fully constrained by the observations and remain model dependent.

In addition to explaining the FBQS 1044 observations, this picture may be relevant to the interpretation of absorption features in similar objects where single-phase models imply a large distance. For instance, in the case of the radio-loud galaxy 3C 191, absorber distances of ~ 28 kpc were inferred by Hamann et al. (2001) using similar arguments to those employed by dK01. A multiple-phase model could place these absorbers much closer to the central source.

This interpretation may also be applicable to other AGN observations. As outlined in § 1, several distinct outflow components have been inferred in various types of AGNs. There is now growing evidence that these components may not be single-phase. For the warm-absorber component, which has been inferred to give rise to both X-ray and UV absorption (e.g., Crenshaw 1997; Mathur et al. 1998; Monier et al. 2001), there are indications in at least some sources that the X-ray and UV absorbing components are not identical (e.g., the Seyfert 1 galaxy NGC 3783 — Kaspi et al. 2000; Kraemer, Crenshaw, & Gabel 2001). Furthermore, it appears that the UV and X-ray absorbing components are themselves divided into multiple zones. In the UV regime, this has been established in Seyfert 1 galaxies like NGC 3783 (Kraemer, et al. 2001) and NGC 3227 (Crenshaw et al. 2001). In the X-ray regime, this is exemplified by the Seyfert 1 galaxy MCG-6-30-15, which was modeled by Morales, Fabian, & Reynolds (2000) as an extended

multi-zone medium. These authors suggested that, in reality, these zones may correspond to a continuum of clouds at different radii and different densities, as in the BELR model of Baldwin et al. (1995). A hierarchical, turbulent-gas realization of this concept was recently presented by Bottorff & Ferland (2001). Our "clouds in a continuous wind" scenario is designed to explicitly address the outflowing nature of the absorbing gas but is otherwise similar to the above picture in its description of spatially coexisting multiple phases. For simplicity, we have treated the clouds as long-lived, pressure-confined entities, but it is entirely conceivable that the clouds are transient features that arise in a turbulent outflow. The same basic picture of a multiphase medium may thus apply to the gas in the BELR, the BALR (e.g., Arav et al. 1999), the warm absorber, and even the NLR (e.g., Komossa 2001).

In conclusion, we have argued that the observations of FBQS 1044 can be interpreted in the context of the standard BALR picture in terms of a gas outflow that consists of (at least) two phases, which we modeled as a continuous wind with embedded dense clouds, shielded from the central continuum. If the shield is identified with the continuous component, then only a fraction of it can be outflowing at a speed that approaches (or exceeds) the value in the Fe/Mg absorption region. We also deduced that the clouds are dusty but that the shield is effectively dust free. As far as we are aware, this is the first instance of a BALR outflow in which the data provide direct evidence for the existence of a multiphase medium. Together with other pieces of evidence, this result lends support to the view that all the major outflow components in AGNs may contain multiple phases.

We gratefully acknowledge the initial work of and continued discussions with Martijn de Kool as well as helpful comments from Mike Brotherton, Abraham Loeb, and the referee. J.E. and A.K. thank NASA for support through grant NAG5-9063.

REFERENCES

Arav, N., Li, Z.-Y., & Begelman, M.C. 1994, ApJ, 432, 62
Arav, N., Korista, K.T., de Kool, M., Junkkarinen, V.T., Begelman, M.C. 1999, ApJ, 516, 27 Z.-Y., & Begelman, M.C. 1994, ApJ, 432, 62
Baldwin, J, Ferland, G., Korista, K., Verner, D., ApJ, 455, L119
Blandford, R.D. 2001, Phil. Trans. R. Soc. Lond. A, 358, 811
Blandford, R.D., & McKee, C. F. 1982, ApJ, 255, 419
Blandford, R.D., & Payne, D.G. 1982, MNRAS, 199, 883
Bottorff, M., Ferland, G. 2001, ApJ, 549, 118
Bottorff, M.C., Korista, K.T., & Shlosman, I. 2000, ApJ, 537, 134
Crenshaw, D.M. 1997, in ASP Conf. Ser. 128, Mass Ejection from AGN, ed. N. Arav, I. Shlosman, & R.J. Weymann (San Francisco: ASP), 121
Crenshaw, D.M., Kraemer, S.B., Bruhweiler, F.C., & Ruiz, J.R. 2001, ApJ, 555, 633
de Kool, M., Arav, N., Becker, R.H., Gregg, M.D., White, R.L., Laurent-Muehleisen, S.A., Price, T., Korista, K.T. 2001, ApJ, 548, 609 (dK01)
Emmering, R.T., Blandford, R.D., Shlosman, I. 1992, ApJ, 385, 460
Everett, J.E., Königl, A., & Kartje, J.F. 2001, in ASP Conf. Ser. 224, Probing the Physics of AGN by Multiwavelength Monitoring, ed. B.M. Peterson, R.S. Polidan, & R.W. Pogge (San Francisco: ASP), 441
Ferland, G.J. 2000, Hazy, A Brief Introduction to Cloudy 94.00
Hamann, F.W., Barlow,T.A., Chaffee, F.C., Foltz, C.B., Weymann, R.J. 2001, ApJ, 550, 142
Kartje J.F., Königl, A., & Elitzur, M. 1999, ApJ, 513, 180
Kaspi, S., Brandt, W.N., Netzer, H., Sambruna, R., Chartas, G., Garmire, G., Nousek, J 2000, ApJ, 535, L17
Königl, A., & Kartje, J.F. 1994, ApJ, 434, 446
Komossa, S. 2001, A&A, 371, 507
Kraemer, S.B., Crenshaw, D.M., & Gabel, J.R. 2001, ApJ, 557, 30
Mathews, W.G. & Ferland, G.J. 1987, ApJ, 323, 456
Mathis, J. S., Rumpl, W., Nordsieck, K. H. 1977, ApJ, 217, 425 (MRN)
Mathur, S., Wilkes, B., & Elvis, M. 1998, ApJ, 503, L23
Monier, E.M., Mathur, S., Wilkes, B., & Elvis, M. 2001, ApJ, 559, 675
Morales, R., Fabian, A.C., Reynolds, C.S. 2000, MNRAS, 315, 149
Murray, N., Chiang, J., Grossman, S. A., Voit, G. M. 1995, ApJ, 451, 498
Netzer, H., & Peterson, B.M. 1997, in "Astronomical Time Series," ed. D. Maoz, A. Sternberg, & E.M. Leibowitz (Dordrecht: Kluwer), 8
Proga, D., Stone, J., Kallman, T.R. 2000, ApJ, 543, 686
Shlosman, I. & Begelman, M.C. 1987, Nature, 329, 29
Tielens, A.G.G.M., McKee, C.F., Seab, C.G., Hollenbach, D.J. 1994, ApJ, 431, 321
Turnshek, D.A. 1988 in Proc. STScI Symp. 2, QSO Absorption Lines:Probing the Universe, ed. S.C. Blades, D.A. Turnshek, & C.A. Norman (Cambridge: Cambridge Univ. Press), 17
Voit, G.M., Weymann, R.J., & Korista K.T. 1993, ApJ, 413, 95
Weymann, R.J. 1997, in ASP Conf. Ser. 128, Mass Ejection from AGN, ed. N. Arav, I. Shlosman, & R.J. Weymann (San Francisco: ASP), 3
Weymann, R.J., Morris, S.L., Foltz, C.B., & Hewett, P.C. 1991, ApJ, 373, 23

TABLE 1
COMPARISON OF THE TWO-PHASE OUTFLOW MODEL WITH OBSERVATIONAL RESULTS FOR FIRST QSO 1044+3656

Quantity	Observational Result	Model Result
N(Fe II)	$\sim 3\times10^{15}$cm^{-2}	3×10^{15}cm^{-2}
N(Fe I)	$< 10^{13}$cm^{-2}	2.5×10^{11}cm^{-2}
N(Mg II)/N(Mg I)	$\gtrsim 30$	500
N(Mg I)	$\sim 2\times10^{13}$cm^{-2}	2×10^{13}cm^{-2}
n_e	~ 4000	4000
A_{2500}	$\lesssim 1$	~ 0.5

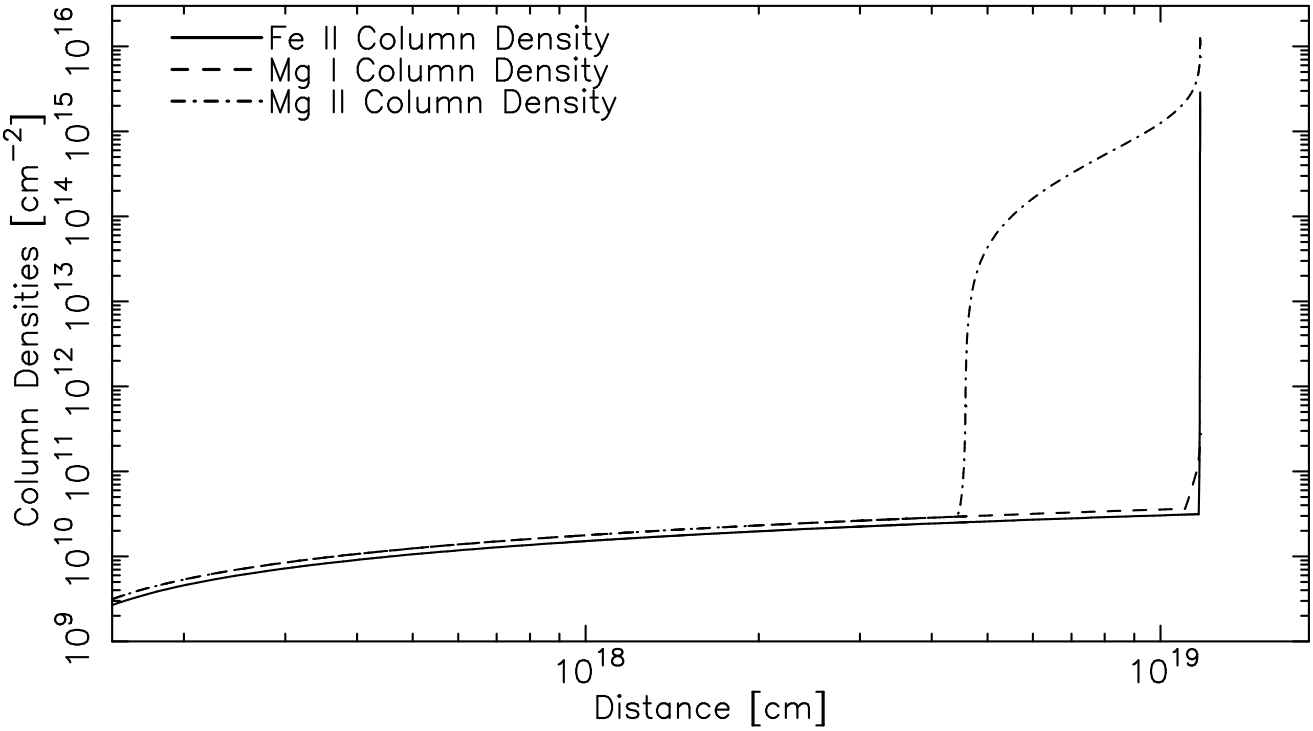

FIG. 1.— Column densities in the dust-free continuous wind model parameterized by $n_{w,i} \approx 10^{8.75}$ cm^{-3}. The continuous wind accounts for the Fe II as well as the higher-velocity Mg II absorption without overproducing the low-ionization Mg I absorption (which is attributed to the dense clouds).

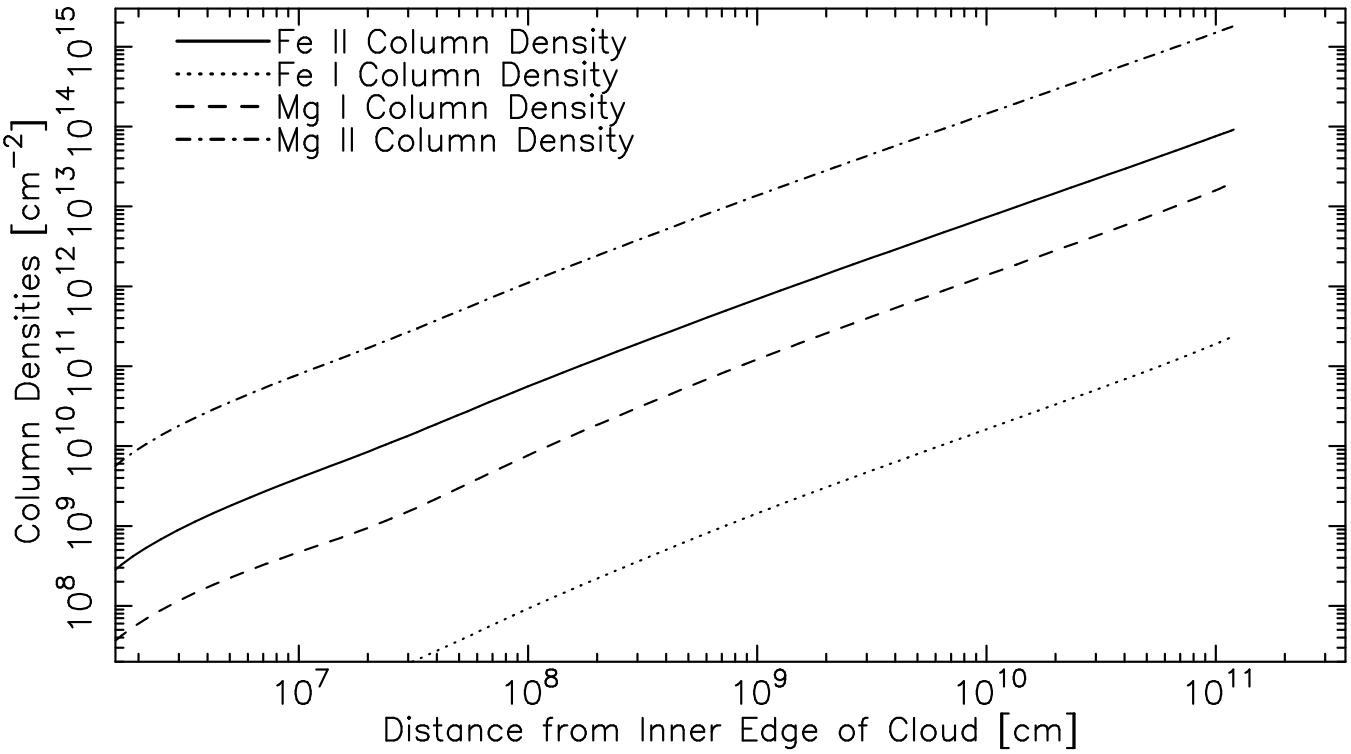

FIG. 2.— Column densities in dusty clouds of hydrogen density $n_c = 10^{8.5}$ cm^{-3} that are shielded by the continuous dust-free wind of Fig. 1. The clouds account for the Mg I absorption without overproducing the higher-ionization Fe II absorption (which is attributed to the continuous wind).